CHAPTER-7

Highly efficient Metal Nanoparticles immobilized on amino-functionalized reduced Graphene Oxide-based bifunctional Catalysts for One-pot multi-steps Henry-Michael

[7.1] Introduction

To satisfy the necessity of sustainable development, the research community from throughout the world are looking for the high atomic utilization rate, simpler operation, reduce in reaction time, work up procedures, low cost, and also for minimizing the chemical wastes that are likely to result from the reactions and to accomplish chemical transformations. To achieve these aims, the multistep chemical conversions in one-pot known as a tandem, domino or cascade reactions have emerged as significant and effectual to chemical synthesis owing to the unique catalytic reactivity and the capability for rapid construction of molecular complexity from simple and readily available starting materials. [1-6]

Nowadays, the multistep reactions are to be synthesized possibly in the single vessel without separating intermediary products and can be catalyzed by multifunctional catalysts has attracted much attention in the field of materials sciences and modern organic synthesis. Conventionally, this multistep one-pot reaction is operated under soluble catalysts (homogeneous systems) such as organic or inorganic bases and Lewis acids, which are suffering from high cost and monotonous catalyst separation procedure, lead to serious economical and environmental problems. To overcome this troublesome, highly efficient heterogeneous catalyst is one of the preferred choices for their remarkable advantages of simpler operation, easier separation, less toxicity, and easier recycling. In this context, numerous heterogeneous multifunctional catalysts i.e. Brønsted acid-Lewis acid, acid-base, acid-metal, and base-metal systems have invoked for the multistep one-pot reaction and provide diverse products with desired yields. [7]

In consequence of the characteristics of simple operations and process escalation, nowadays, scientists have paid a great deal of attention on the development of one-pot and/or tandem organic reactions. [9-11] Despite the various homogeneous systems designed to gratify this idea, barely any such homogeneous systems have been developed so far consisting of bifunctional acid-base catalysts which are required primarily for the one-pot reactions. This is because of both acid and base sites are easily deactivated each other in such

systems. Consequently, the growth of supported catalysts especially consisting of both acid and base bifunctional active sites that can efficiently promote the one-pot reactions have nowadays received great interests. [12-18] The acidic and basic functions can activate electrophiles and nucleophiles, respectively and therefore, the combination of acid and base catalysts is believed to be an eye-catching approach for the tandem reactions. [15; 19-25] Recently, a series of tandem reactions have been reported by utilizing acid-base bifunctional catalysts hosted on the solid matrixes [22]. For instance, Angeletti group [22] have prepared a bifunctional system consists of silanols from MCM-41 providing acidic sites, however, the 1,8-bis(dimethylamino)naphthalene functional groups embedded therein gives basic sites useful in acid-base tandem reactions. Davis [26] and Shanks groups [27] have examined supported acid-base catalysts utilizing an aminopropyl-functionalized mesosilica, SO_3H-SBA-15. Besides, the amino group-functionalized metal-organic framework (MOF), MIL-101(Al)-NH_2, have also been synthesized via the solvothermal method and tested over tandem deacetalization-Knoevenagel condensation reaction as a bifunctional acid-base catalyst. [28] The NH_2-functionalized graphene oxide including carboxylic acid was synthesized using a single-step silylation approach and employed as a bifunctional catalyst. [29] D. Wang group [30] have explored a hierarchical core/shell structured acid-base bifunctional catalyst, ZSM-5@$Mg_3Si_4O_9(OH)_4$ using a hydrothermal reaction between the silica species on ZSM-5 surface and the Mg^{2+} source in basic solution and employed for one-pot deacetalization-Knoevenagel condensation reaction.

In recent times, carbonaceous support has been paid much consideration especially in electrocatalysis and material science owing to its beneficial nature, porous structure, greater stability, environmental acceptability and low cost. Among the carbonaceous materials, in the last 2-3 decades, graphene has received widespread research attention due to its mesmerizing characteristics such as its profusion, densely packed hexagonal honeycomb sp^2 hybridized 2D lattice, lightweight, exceptional large surface area (2630 m^2g^{-1}), high electrical conductivity and thermal stability as well as inertness to supported metals.

Besides this, it also possesses high tensile and mechanical strengths, making them stronger and able to bind with versatile aromatic/aliphatic bases and/or Lewis acids or both either through immobilized on the surface or through the covalent attachment or tethering. Taking advantage of these unique features of functionalized graphene-based materials is not only accelerating the reaction rate but also improving the selectivity for the desired product.

Herein, we report a simple, convenient and highly efficient Lewis acid metal ions/oxides immobilized on amino-functionalized reduced graphene oxide-based bifunctional catalysts (MNPs/Am@rGO) [Where, MNPs = Fe or Nb_2O_5; Am = *p*-phenylenediamine (PPD) and/or ethylene diamine (ED)]. The catalytic aptitude of these bifunctional catalysts has been tested over the one-pot multi-steps Henry-Michael reaction using different aromatic aldehydes, nitromethane, malononitrile and/or nucleophilic compounds. The effect of varying parameters influencing the catalytic activity such as catalyst amount, mole ratio, solvent, temperature, and time have also been screened.

[7.2] Experimental section

a) Materials

Malononitrile (MLN), ethyl cyanoacetate, methyl acetoacetates and ethyl acetoacetate was procured from Spectrochem Pvt. Ltd. $NbCl_5$, $FeCl_3$ anhydrous, ethylenediamine, $NaBH_4$, were procured from S D Fine Chem Ltd. *p*-Phenylenediamine was purchased from High Purity Laboratory Chemicals Pvt. Ltd. All the materials are of analytical grade and used as received without further purification.

b) Synthesis of graphene oxide (GO)

GO was prepared from graphite flakes using a modified Hummers' method as already discussed in Chapter 2.

c) Synthesis of amino modified graphene oxide (Am@GO) nanocatalyst

To functionalize the carboxyl groups of GO nanosheet, Go was treated with *p*-phenylenediamine (PPD) and/or ethylene diamine (ED). Dispersion of 500 mg of GO in 100 mL of distilled water was ultrasonicated for 10 min. Then, 1 g of *p*-phenylenediamine and/or ethylenediamine in 10 mL of acetone was added

slowly in the suspension of GO and the suspension mixture was kept to stir for 12 h at room temperature. The resulting solid product was isolated by centrifugation and the product was washed with acetone and water which was later dried in a vacuum oven for 48 h.

d) Synthesis of FeNPs/Am@rGO nanocatalysts

As-synthesized Am@GO viz. PPD@GO and/or ED@GO was taken (20 mg) in 10 mL of distilled water and then ultrasonicated for 30 min at room temperature. It was followed by a slow addition of 2 mmol of an aqueous solution of $FeCl_3$ into the suspension of Am@GO which was ultrasonicated for 20 min to generate homogeneously dispersed suspension. After being sonicated, a freshly prepared solution of $NaBH_4$ (5 mL) was added drop by drop into the suspension and solution mixture was kept at room temperature and stirred constantly for 30 min. Finally, black precipitates of nanocomposite materials were formed, maybe indicating the successful reduction of Fe to FeNPs and GO to rGO. The solid product was isolated by centrifugation and washed with distilled water, later dried in an air oven at 65 ^{o}C.

e) Synthesis of Nb_2O_5/Am@rGO nanocatalysts

In a typical synthesis process, as-prepared 20 mg Am@GO viz. PPD@GO and/or ED@GO was dispersed in 10 mL of distilled water and sonicated for 3 h. Then 0.1 g of $NbCl_5$ was added and stirred using a magnetic stirrer. It was followed by adding of 2 mmol of $NbCl_5$ into the suspension of Am@GO and ultrasonicated for 20 min to generate homogeneously dispersed suspension. After completed sonicated, a freshly prepared solution of $NaBH_4$ (5 mL) was added drop by drop into the suspension and solution mixture was stirred constantly for 30 min at room temperature. The solution was transferred to an autoclave and heated at 413 K at 6 h. The autoclave was cooled down to ambient temperature naturally, the solid product was separated by centrifuge and washed with distilled water, ethanol several times followed by drying in an air oven at 65 ^{o}C.

f) Catalytic test

In a typical run of one-pot Henry-Michael reaction, a mixture of 5 mmol benzaldehyde, 5 mmol nitromethane, 5 mL toluene and 80 mg of catalyst were

taken into a 50 mL round bottom flask and the reaction mixture was heated to 50 ^{o}C for 2 h under vigorous stirring. Then, the reaction temperature was cooled to 40 ^{o}C. After that 7.5 mmol of malononitrile was added to the mixture and allowed to stir for another 3 h. The catalyst was isolated by centrifugation. The organic aliquot was analyzed by high-performance liquid chromatography (HPLC, Agilent 6410B). The catalyst was recovered by washing with ethanol followed by distilled water and later on dried in a hot air oven at 80 ^{o}C for 6 h before reuse.

[7.3] Results and discussion

Indeed, before we checked the catalytic aptitude of as-prepared bifunctional catalysts for the one-pot Henry-Michael reaction, it is requisite to understand the chemical arrangements and structural morphologies of the as-synthesized bifunctional catalysts. These supported catalysts were corroborated through the various physicochemical techniques as discussed below:

Characterization of nanocatalyst:

(a) Raman spectra:

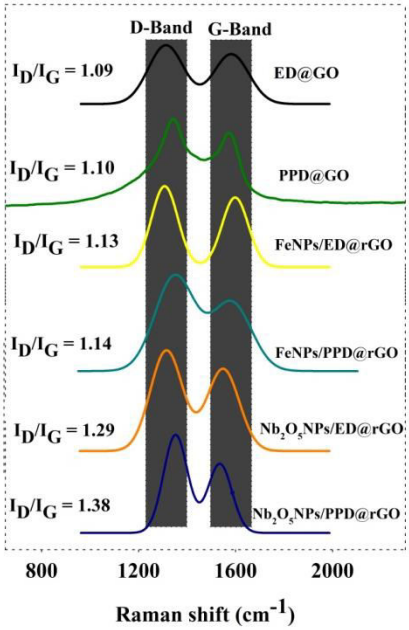

Figure 1 Raman spectra of ED@GO, PPD@GO, FeNPs/ED@rGO, FeNPs/PPD@rGO, Nb_2O_5NPs/ED@rGO, and Nb_2O_5NPs/PPD@rGO

The lattice structure and morphological changes throughout the synthesis of nanocatalysts were investigated by the Raman spectroscopy. The Raman spectra of ED@GO, PPD@GO, FeNPs/ED@rGO, FeNPs/PPD@rGO, Nb_2O_5NPs/ED@rGO, and Nb_2O_5NPs/PPD@rGO samples have demonstrated in Fig. 1. Two distinguished peaks observed at ~1320 and ~1556 cm^{-1} are assigned to the symmetry forbidden of the longitudinal plane phonon vibration or k-point phonons of A_{1g} symmetry (D-band) and the long-wavelength longitudinal phonon mode of graphene (E_{2g} phonon) (G-band) occurs due to the sp^2 carbon network of the graphene plane, respectively [31]. In addition to this, the intensity ratio (I_D/I_G) for GO observed to be 0.99 (Chapter 2, Fig. 10), however, it was increased up to 1.09, 1.10, 1.13, 1.14, 1.29, and 1.38 for ED@GO, PPD@GO, FNPs/ED@rGO, FeNPs/PPD@rGO, Nb_2O_5NPs/ED@rGO, and Nb_2O_5NPs/PPD@rGO, respectively. This enhancing intensity ratio might be due to the inclusion of amino moieties and metal ions on the surface of the rGO nanosheet. In addition, we have estimated the crystalline size of the as-prepared nanocatalysts by using the Tuinstra–Koenig relation. With this equation, the inter defect distance estimated to be 15.37, 15.23, 14.82, 14.69, 12.99, and 12.14 nm for ED@GO, PPD@GO, FeNPs/ED@rGO, FeNPs/PPD@rGO, Nb_2O_5NPs/ED@rGO, and Nb_2O_5NPs/PPD@rGO catalyst, respectively. [32]

(b) Fourier transform infrared spectroscopy

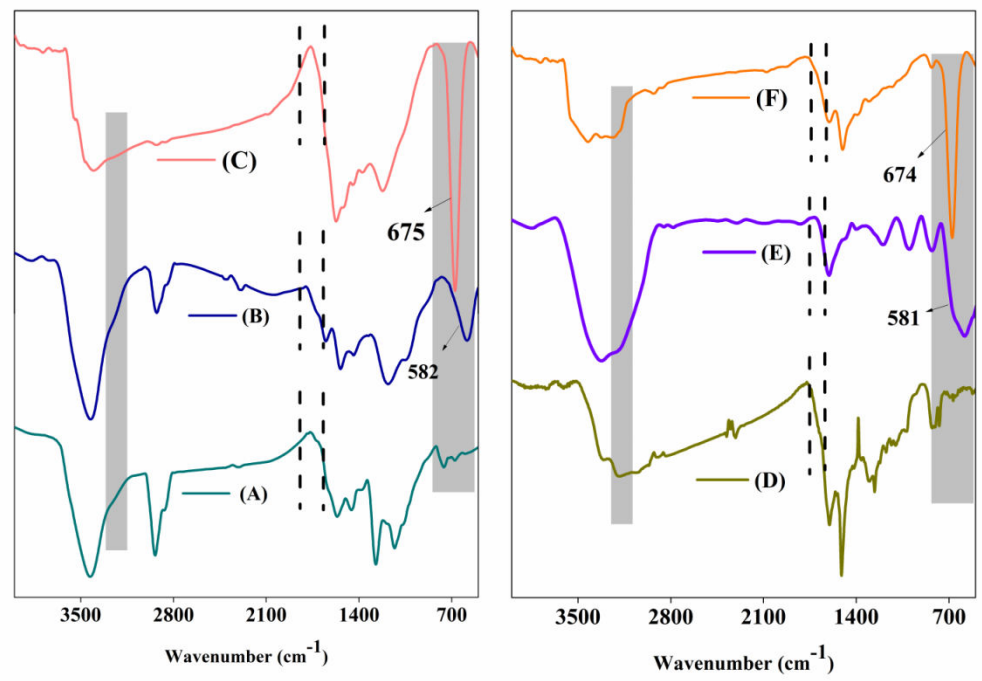

Figure 2 FTIR spectra of (A) ED@GO, (B) FeNPs/ED@rGO, (C)Nb_2O_5NPs/ED@rGO (D) PPD@GO, (E) FeNPs/PPD@rGO, and (F) Nb_2O_5NPs/PPD@rGO.

The FTIR spectra of PPD@GO, ED@GO, Nb_2O_5NPs@PPD/GO, Nb_2O_5NPs@ED/GO, FeNPs@PPD/GO, FeNPs@ED/GO are depicted in Figure 2. In FTIR spectra of PPD@GO, ED@GO, Nb_2O_5NPs@PPD/GO, Nb_2O_5NPs@ED/GO, FeNPs@PPD/GO, FeNPs@ED/GO, two bands were observed at 3246–3181 cm^{-1} and 2863–2893 cm^{-1}, which are indicated to ν(N–H) and ν(C–H) aromatic stretching vibrations, respectively, however, ν(C=C) stretching vibration examined at ~1598 cm^{-1} [33]. The presence of stretching vibration at 1306 and 1308 cm^{-1} are assigned to the C–N groups in ED@GO and PPD@GO, respectively. However, after the immobilization of metal ions (Fe and Nb) on the surface of Am@GO (where Am = ED or PPD) nanosheets, the said band was shifted to lower frequency region (i.e. in the spectra of FeNPs/ED@rGO, FeNPs/PPD@rGO, Nb_2O_5NPs/ED@rGO, Nb_2O_5NPs/PPD@rGO). In addition to this, two new peaks observed at ~580 and ~675 cm^{-1}, indicating the stretching vibrations of the Fe-O and Nb-O, respectively. Moreover, the ν(C=O) band observed in the region of 1720-1722

cm^{-1} (Chapter 2, Fig. 6), was disappeared in the spectra of ED@GO and PPD@GO, suggesting the successful functionalizing of amino groups of ethylenediamine and *p*-phenylenediamine derivatives on the surface of GO through the functionalization of –COOH groups. [34]

(c) High resolution Transmission electron microscopy (HR-TEM):

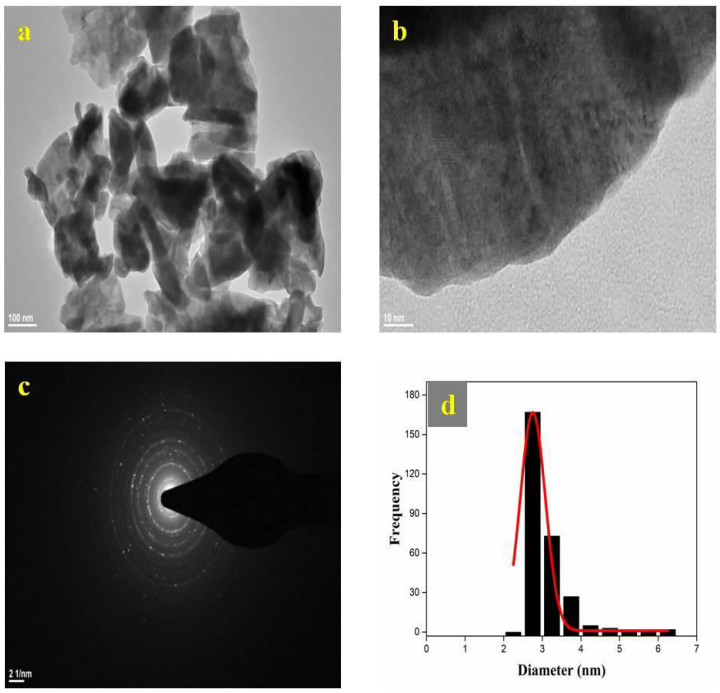

Figure 3 HR-TEM images of (a) Nb_2O_5NPs/PPD@rGO (b) Nb_2O_5NPs/PPD@rGO with fringe spacing, (c) SAED image of Nb_2O_5NPs/PPD@rGO, (d) Histogram graph of Nb nanoparticles

In order to highlight microstructural features (size, microstructure, and spherical morphology, SAED pattern) in detail, HRTEM analysis of Nb_2O_5NPs/PPD@GO sample was performed and their corresponding images with electron diffraction patterns are illustrated in Fig. 3. As shown in Fig. 3(a), the fine narrow size of Nb_2O_5 nanoparticles with nano-rod type shape was dispersed on PPD@GO nanosheet. As can be seen in Fig. 3(b), the existence of lattice fringe patterns suggesting the shape of the crystalline nanorods shape of the as-prepared catalyst. The adjacent lattice fringes were observed to be 2.7 ± 0.34 Å, which is in accordance with the interplanar spacing of the crystal planes. The diffraction spots

were monitored in the SAED image of Nb_2O_5NPs/PPD@rGO [Fig. 3(c)] confirmed the intense spherical spots of Nb_2O_5 observed in SAED pattern, are corresponds to the XRD results.

(d) X-ray diffraction study

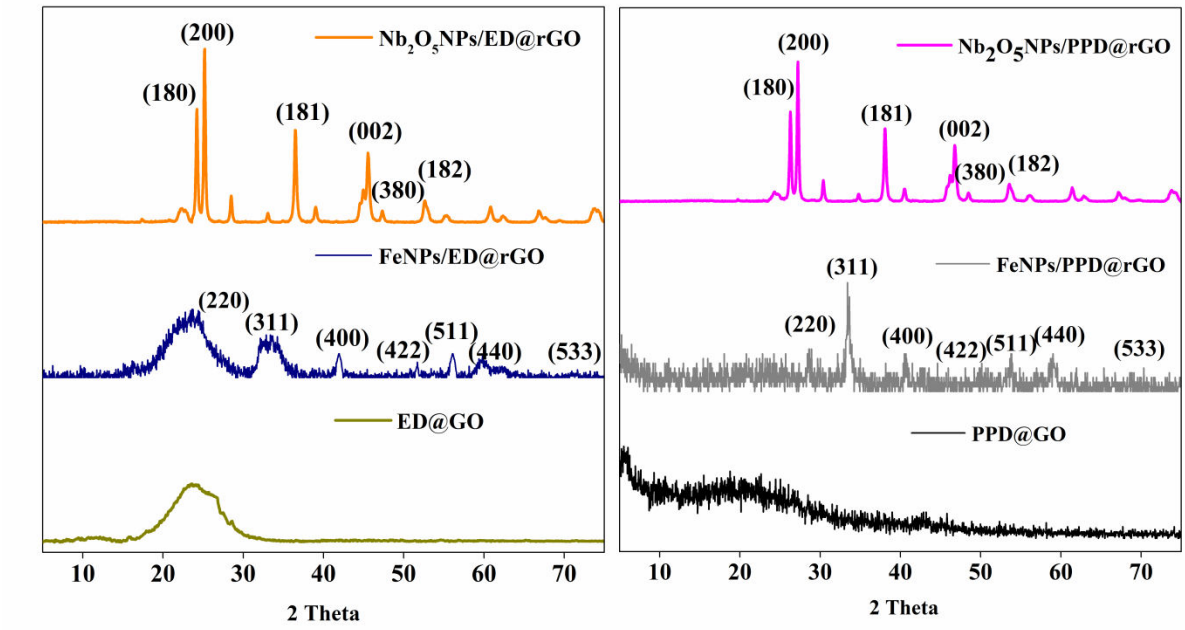

Figure 4 XRD pattern of ED@GO, PPD@GO, FeNPs/ED@rGO, FeNPs/PPD@rGO, Nb_2O_5NPs/ED@rGO, and Nb_2O_5NPs/PPD@rGO.

XRD patterns of the as-prepared samples viz. ED@GO, PPD@GO, FeNPs/ED@rGO, FeNPs/PPD@rGO, Nb_2O_5NPs/ED@rGO, Nb_2O_5NPs/PPD@rGO are demonstrated in Fig. 4. [35-37] The XRD patterns of GO sample is shown in chapter 2, Fig. 8 which compared with XRD pattern of ED@GO and PPD@GO. A notable peak is observed at $2\theta = 26.3°$, suggesting the stitching of the GO layers occurred during the preparation of ED@GO and PPD@GO samples by ethylene diamine and *p*-phenylenediamine. Furthermore, as shown in Fig. 4 all the reflection peaks of the XRD pattern (i.e. FeNPs/ED@rGO, FeNPs/PPD@rGO, Nb_2O_5NPs/ED@rGO, Nb_2O_5NPs/PPD@rGO) can be indexed to the crystallinity of Fe nanoparticles compared with JCPDS standard 19-0629 of Fe and highly crystalline orthorhombic phase of Nb_2O_5 utterly matched with JCPDS 30-0873 of Nb_2O_5. From the XRD results confirmed that the successful

immobilization of Fe and Nb_2O_5 nanoparticles on the surface of amino-functionalized GO nanosheets.

(e) Thermogravimetric study

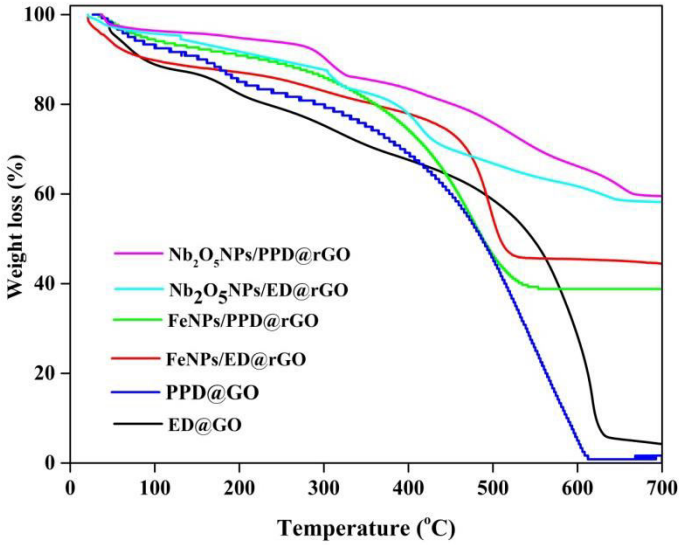

Figure 5 TGA analysis of ED@GO, PPD@GO, FeNPs/ED@rGO, FeNPs/PPD@rGO, Nb_2O_5NPs/ED@rGO, and Nb_2O_5NPs/PPD@rGO

The quantitative estimation of organic content and framework stability of the as-prepared ED@GO, PPD@GO, FeNPs/ED@GO, FeNPs/PPD@GO, Nb_2O_5NPs/ED@GO, Nb_2O_5NPs/PPD@rGO samples were investigated through the thermogravimetric (TG) analyses (Fig. 5). The thermograms of as-synthesized ED@GO and PPD@GO samples are shown weight losses in three steps: The initial weight losses of 6.4% and 6.7%, respectively observed in the temperature range of 40–110 ^oC, believed to be due to the liberation of trapped water molecules. The second (from ~110–280°C) and third (from ~280–650°C) steps are supposed to be due to the decompositions of oxygen-containing functional groups and the carbon skeleton, respectively. The observed weight losses for ED@GO and PPD@GO in these temperature ranges are 11.0, 11.4% and 71.7, 79.6%, respectively.

Moreover, during *in situ* grafting of Fe and Nb_2O_5 nanoparticles on the amino-functionalized GO nanosheets have shown two steps degradation patterns

(Fig. 5). The initial degradation occurs in the temperature range of ~110-280 ^{o}C (for FeNPs/ED@rGO, FeNPs/PPD@rGO, Nb_2O_5NPs/ED@rGO, and Nb_2O_5NPs/PPD@rGO samples) with observed mass losses of 5.4, 8.2, 7.3, 8.4 %, respectively assigned to the decomposition of oxygen-containing functional groups. However, the second weight losses (i.e. 38.7, 48.2, 30.1, 31.4%) of the aforesaid samples observed in the temperature range of 280-650 ^{o}C, might be attributing to the degradation of the carbon skeletons.

[7.4] Catalytic reaction

After end-up with the detailed characterization of as-prepared samples through varying physicochemical techniques, herein we discussed the catalytic aptitude of the as-synthesized catalysts over one-pot multi-steps Henry-Michael reaction using benzaldehyde, nitro-methane and malononitrile as starting reagents. Moreover, the impact of distinct parameters such as various catalytic systems, catalyst loading, varying solvents, and varying time influencing catalytic activity has also been studied.

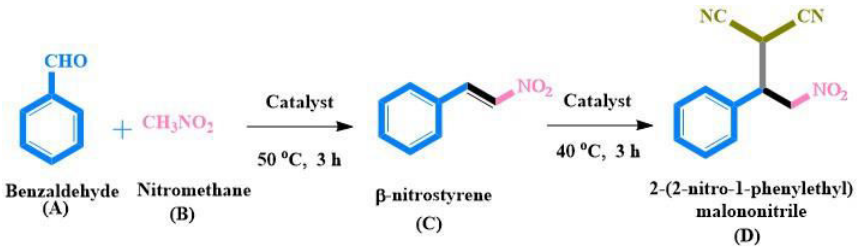

Scheme 1 A schematic representation of Henry-Michael reaction.

The catalytic aptitude of the as-prepared nanocatalysts was performed over one-pot multi-steps Henry-Michael reaction. To acquire this, first, all the catalytic systems like graphite flakes, GO, ED, PPD, ED@GO, PPD@GO, FeNPs/ED@rGO, FeNPs/PPD@rGO, Nb_2O_5/ED@rGO, and Nb_2O_5/PPD@rGO were employed to get your hands on the most appropriate catalyst for the aforesaid one-pot reaction and the results are illustrated in Table 1. As shown in Table 1, pure graphite flakes, GO and without catalyst have shown diminutive or lesser results. On the other hand, the unsupported ED and PPD systems as base catalysts have given mild to moderate conversions of benzaldehyde i.e. 35.6% and 41.9%, respectively. However, such systems may be facing of recyclability

issues. For that reason, we have grafted ED and/or PPD on the surface of GO as base catalysts, showing significant results of benzaldehyde conversions viz. 79.8% and 81.8%, respectively. In addition, we immobilized Fe and/or Nb_2O_5 NPs on the amino-functionalized GO as bifunctional catalysts which have further boosted up the results showing both exceptional conversions and selectivity (Table 1). The immobilization of metal nanoparticles (Fe and/or Nb_2O_5 NPs) worked as Lewis acid sites which activates the carbonyl partner of benzaldehyde substrate and the bifunctional catalyst (a combination of both Lewis acid-Bronsted base) that activates and brings both reactants together. As shown in Table 1, among the various catalytic systems, Nb_2O_5NPs/PPD@rGO has preferred as a representative catalyst showing excellent conversions of benzaldehyde (A) (90.6%) and β-nitrostyrene (C) (88.9%) with prominent 2-(2-nitro-phenylethyl)malononitrile (D) selectivity of 93.2%. Hence, this catalyst has chosen for further studies. [38]

Table 1 Catalytic performance of synthesized catalysts over the one-pot Henry-Michael reaction.

No.	Various catalytic systems	Conversion of Benzaldehyde (A) (%)	Conversion of β-nitrostyrene (C) (%)	Selectivity of 2-(2-nitro-phenylethyl) malononitrile (D) (%)
1	Without catalyst	4.6	3.7	3.3
2	Graphite	5.9	5.3	3.9
3	GO	18.2	14.4	11.4
4	ED	35.6	33.2	41.9
5	PPD	41.9	38.7	50.8
6	ED@GO	79.8	74.3	81.6
7	PPD@GO	81.8	79.6	82.9
8	FeNPs/ED@rGO	84.5	82.9	88.2
9	FeNPs/PPD@rGO	87.9	84.4	91.6

10	Nb_2O_5NPs/ED@rGO	86.1	85.2	88.4
11	Nb_2O_5NPs/PPD@rGO	90.6	88.9	93.2

Reaction conditions for one-pot multi-steps reaction: benzaldehyde (5 mmol), nitromethane (5 mmol), malononitrile (7.5 mmol) varying catalysts (80 mg), toluene (5 mL), temp. (50 ^oC for first step; 40 ^oC for second step), Time (3 h for first step; 3 h for second step).

a) Effect of catalyst dosage

The catalyst dosage is one of the significant factors in one-pot multi-steps Henry-Michael reaction. As shown in Table 2, four different dosages viz. 60, 70, 80, and 90 mg of Nb_2O_5NPs/PPD@rGO were used. Among them, the utmost of 90.6% benzaldehyde conversion (in the first step) and 88.9% of β-nitrostyrene (in the second step) with 93.2% of 2-(2-nitro-phenylethyl)malononitrile selectivity was monitored with 80 mg of catalyst dosage. A further rise in the catalyst dosage from 80 to 90 mg observed no noteworthy difference in conversion but the selectivity of 2-(2-nitro-phenylethyl)malononitrile was declined to some extent i.e. 88.1% (Table 2), conceivably due to the formation of by-products. Hence, the best possible dosage of the catalyst is preferred to be 80 mg for further studies.

Table 2 The catalytic performance of Nb_2O_5NPs/PPD@rGO as a representative catalyst with varying dosages over the One-Pot Henry-Michael reaction

No.	**Catalyst amount**	**Conversion of Benzaldehyde (A) (%)**	**Conversion of β-nitrostyrene (C) (%)**	**Selectivity of 2-(2-nitro-phenylethyl) malononitrile (D) (%)**
1	60	77.4	75.1	80.9
2	70	83.5	82.6	85.1
3	80	90.6	88.9	93.2
4	90	90.9	88.9	88.1

Reaction conditions for one-pot multi-steps reaction: benzaldehyde (5 mmol), nitromethane (5 mmol), malononitrile (7.5 mmol) varying catalyst dosages (**X**

mg), toluene (5 mL), temp. (50 ^{o}C for first step; 40 ^{o}C for second step), Time (3 h for first step, 3 h for second step).

b) Effect of Solvents

The upshot of discrete solvents such as polar protic (methanol), polar aprotic (acetonitrile), and non-polar (toluene) was studied for this one-pot multi-steps Henry-Michael reaction with keeping other parameters fixed. As shown in Table 3, conversions of benzaldehyde and β-nitrostyrene with 2-(2-nitro-phenylethyl)malononitrile selectivity were observed to be decreasing in the order of: toluene (90.6%, 88.9% and 93.2%, respectively) > methanol (75.3%, 73.6% and 65.1%, respectively) > acetonitrile (73.6%, 71.9% and 55.6%, respectively). Among them, toluene with unrivalled dilution factor gives superior conversions and selectivity. Hence, we preferred toluene as a representative solvent for further experiments. [39]

Table 3 Catalytic performance of various solvents over the One-Pot Henry-Michael reaction

No.	Solvents	Conversion of Benzaldehyde (A) (%)	Conversion of β-nitrostyrene (C) (%)	Selectivity of 2-(2-nitro-phenylethyl) malononitrile (D) (%)
1	Methanol	75.3	73.6	65.1
2	Acetnitrile	73.6	71.9	55.6
3	Toluene	90.6	88.9	93.2

Reaction conditions for one-pot multi-steps reaction: benzaldehyde (5 mmol), nitromethane (5 mmol), malononitrile (7.5 mmol) catalyst (80 mg), varying solvents (5 mL), temp. (50 ^{o}C for first step; 40 ^{o}C for second step), Time (3 h for first step, 3 h for second step).

c) Impact of Time

For a typical one-pot multi-steps Henry-Michael reaction, it is quite important to terminate the reaction at the specific time to get somewhere in achieving higher conversions of benzaldehyde and β-nitrostyrene together with 2-(2-nitro-phenylethyl)malononitrile product selectivity. In this multi-steps

reaction, we have decided to keep the time duration (3 h) fixed for the first step, getting maximum conversion of benzaldehyde (90.6%), However, in the subsequent step, we have executed this reaction at varying time intervals, viz. 1, 2, 3 and 4 h (Table 4). 68.1% conversion of β-nitrostyrene is achieved in the first 1 h but the selectivity for 2-(2-nitro-phenylethyl)malononitrile is found to be 61.6%. On enduring the reaction to 2 h, 78.9% and 65.8% of conversion of β-nitrostyrene and 2-(2-nitro-phenylethyl) malononitrile product selectivity are observed, respectively. Furthermore, when reaction time extends to 3 h, the conversion increased up to 88.9% with 93.2% product selectivity was noticed. On further continuing the reaction up to 4 h, no change in the conversion (88.9%), however, the product selectivity was marginally dropped down (87.6%). Therefore, we have chosen the reaction time as 3 h to achieve other parameters.

Table 4 Catalytic performance of varying time over the One-Pot Henry-Michael reaction

No.	Time	Conversion of Benzaldehyde (A) (%)	Conversion of β-nitrostyrene (C) (%)	Selectivity of 2-(2-nitro-phenylethyl) malononitrile (D) (%)
1	1	71.6	68.1	61.6
2	2	83.6	78.9	65.8
3	3	90.6	88.9	93.2
4	4	90.6	88.9	87.6

Reaction conditions for one-pot multi-steps reaction: benzaldehyde (5 mmol), nitromethane (5 mmol), malononitrile (7.5 mmol) catalyst (80 mg), toluene (5 mL), temp. (50 ^{o}C for first step; 40 ^{o}C for second step), Time (3 h for first step, **X** h for second step).

[7.5] Henry-Michael reaction using different aldehydes over Nb_2O_5NPs/PPD@rGO as a representative nanocatalyst

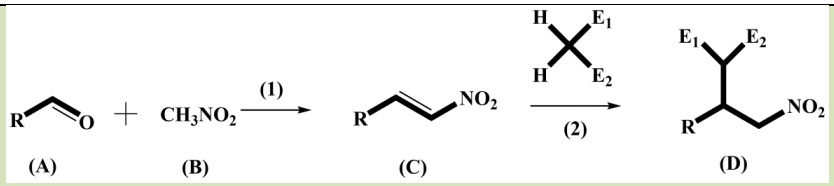

Entry	Substract (A)	Active methylene Compounds		Conversion of (A) (%)	Conversion of (C) (%)	Selectivity of (D) (%)
		E_1	E_2			
1	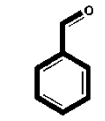	-CN	-CN	90.6	88.9	93.2
2	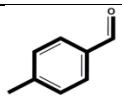	-CN	-CN	85.6	59.07	15.6
3	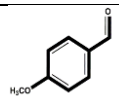	-CN	-CN	85.7	78.9	16.1
4	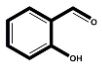	-CN	-CN	81.2	52.3	10.3
5	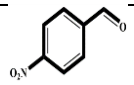	-CN	-CN	80.1	53.3	7.3
6	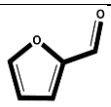	-CN	-CN	88.3	78.9	24.3
7	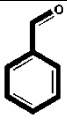	-CN	$-COOCH_2CH_3$	78.9	77.3	73.8

Table 5 The one-pot multi-steps Henry-Michael reaction of diverse substrates over Nb_2O_5 NPs/PPD@rGO as a representative catalyst.

Reaction conditions for one-pot multi-steps reaction: benzaldehyde (5 mmol), nitromethane (5 mmol), malononitrile (7.5 mmol) catalyst (80 mg), toluene (5 mL), temp. (50 ^oC for first step; 40 ^oC for second step), Time (3 h for first step, 3 h for second step).

After achieving the optimized conditions for the aforesaid condensation reaction, we have further been investigated this reaction using diverse range of substrates such as aldehydes, nitromethane and active methylene compounds generating the desired product and its derivative (Table 5). When the reaction was carried out with various aldehydes including electron withdrawing group (i.e. 4-methyl benzaldehyde and/or 4-methoxy benzaldehyde) and/or electron donating group (i.e. 4-nitrobenzaldehyde), nitromethane and active methylene compounds gave the desired product. [40] From the Table, various aromatic aldehydes including electron-withdrawing (like 4-methyl benzaldehyde, 4- methoxy benzaldehyde, effectively coupled with nitro methane and malononitrile to furnish desired product with excellent conversion and selectivity (Table 5, entry 2 and 3). However, 2-hydroxy benzaldehyde and 4-nitrobenzaldehyde observed diminish conversion and selectivity, might be due to the steric impediment factor. (Table 5, entry 4 and 5) In addition to this, we have also carried out heteroatom compound i.e. furfuraldehyde with nitro methane and malononitrile, achieving to the desired conversion (A) with almost good conversion (C) and product selectivity. (Table 5, entry 6). Furthermore, Benzaldehyde treated with nitro methane and ethyl cyano acetate, observing good conversion and selectivity of desired product. (Table 5, entry 7).

[7.6] Recyclability Test

The recovery and reusability of the catalyst are of enormous importance to any heterogeneous catalytic system. The recyclability of Nb_2O_5/PPD@rGO as a representative catalyst was checked over One-Pot Henry-Michael reaction and the results are demonstrated in Table 6. To begin with, the catalyst was separated from the reaction mixture by filtration, washed with distilled water several times followed by oven drying prior to employing for the subsequent catalytic test. For this multi-steps reaction, the conversions of benzaldehyde and β-nitrostyrene with 2-(2-nitro-phenylethyl)malononitrile product selectivity in the fresh run are 90.6%, 88.9% and 93.2%, respectively (Table 6). However, on the whole marginally dropped down in the conversions as well as product selectivity was

noticed after each run (Table 6), this loss of activity was supposed to be caused by metal leaching all through the recovery process and reaction.

Table 6 Recyclability of Nb_2O_5 NPs/PPD@rGO in the one-pot Henry-Michael reaction

No.	Runs	Conversion of Benzaldehyde (A) (%)	Conversion of β-nitrostyrene (C) (%)	Selectivity of 2-(2-nitro-phenylethyl) malononitrile (D) (%)
1	Fresh	90.6	88.9	93.2
2	1st	88.6	82.4	93.2
3	2nd	87.5	82.2	86.5
4	3rd	86.1	80.9	82.8
5	4th	83.1	80.9	75.4

Reaction conditions: benzaldehyde (5 mmol), Nitromethane (5 mmol), malononitrile (7.5 mmol) varying catalysts (80 mg), Solvents (5 mL), temp. (50 ^oC, 40 ^oC), Time (2, 3 h).

[7.7] Conclusion

In concluding annotations, we have adequately developed a graceful and skilled design for the synthesis of transition metal immobilized on amino-functionalized rGO-based bifunctional catalysts (MNPs/Am@rGO) (where M = Fe and/or Nb_2O_5; Am = ED and/or PPD), exhibiting amino-based organic derivatives on rGO nanosheet endowing with basic sites and FeNPs and/or Nb_2O_5 NPs immobilized on the surface of rGO supplying Lewis acidic characteristics. Among them, Nb_2O_5 NPs/PPD@rGO possessed phenomenal catalytic results leading to 90.6% and 88.9% conversions of benzaldehyde and β-nitrostyrene, respectively with 93.2% of 2-(2-nitro-phenylethyl)malononitrile product selectivity in one-pot multi-steps Henry-Michael reaction. This could be attributed to the mutual effects of acid-base sympathetic catalytic aptitude as well as the unique two-dimensional open structure furnished by the rGO nanosheet. These metal nanoparticles immobilized amino-functionalized rGO-based acid-base bifunctional catalysts are expected to provide a tangible plan of new contexts in

the development of more energetic and recyclable heterogeneous multifunctional catalysts for novel chemical transformations.

[7.8] References

[1] D. Damodara, R. Arundhathi, P. R. Likhar, *Adv. Synth. Catal*. **356**, 189 (2014).

[2] A. Bayat, M. Shakourian-Fard, N. Talebloo, M. M. Hashemi, *Appl. Organometal. Chem*. **32**, 4061 (2018).

[3] J. Zheng, J. Qu, H. Lin, Q. Zhang, X. Yuan, Y. Yang, Y. Yuan, *ACS Catal*. **6**, 6662 (2016).

[4] W. Fu, L. Yue, X. Duan, J. Li, G. Lu, *Green Chem*. **18**, 6136 (2016).

[5] H. Xie, Y. Li, L. Huang, F. Nong, G. Ren, T. Fan, Q. Lei, W. Fang, *Dalton Trans*. **45**, 16485 (2016).

[6] H. Chen, S. He, M. Xu, M. Wei, D. G. Evans, X. Duan, *ACS Catal*. **7**, 2735 (2017).

[7] A. Corma, M. Iglesias, F.J. Sanchez, *Chem. Commun*. 1635 (1995).

[8] L. Bui, H. Luo, W.R. Gunther, Y. Roman-Leshkov, *Angew. Chem. Int. Ed.* **52,** 8022 (2013).

[9] J. M. Lee, Y. Na, H. Han, S. Chang, *Chem. Soc. Rev*., **33**, 302 (2004).

[10] J.-C. Wasilke, S. J. Obrey, R. T. Baker, G. C. Bazan, *Chem. Rev.,* **105**, 1001 (2005).

[11] M. J. Climent, A. Corma, S. Iborra, *Chem. Rev*., **111**, 1072 (2011).

[12] F. Gelman, J. Blum, D. Avnir, *J. Am. Chem. Soc*., **124**, 14460 (2002).

[13] A. Corma, T. Ródenas, M. J. Sabater, *J. Catal*., **279**, 319 (2011).

[14] N. R. Shiju, A. H. Alberts, S. Khalid, D. R. Brown, G. Rothenberg, *Angew. Chem. Int. Ed*., **50**, 9615 (2011).

[15] K. Motokura, M. Tada, Y. Iwasawa, *J. Am. Chem. Soc*., **131**, 7944 (2009).

[16] Y. Huang, S. Xu, V. S.-Y. Lin, *Angew. Chem., Int. Ed*., **50**, 661(2011).

[17] M. Sasidharan, S. Fujita, M. Ohashi, Y. Goto, K. Nakashima, S. Inagaki, *Chem. Commun*., **47**, 10422 (2011).

[18] S. J. Broadwater, S. L. Roth, K. E. Price, K. Muris, M. Kobašlija, D. T. McQuade, *Org. Biomol. Chem*., **3**, 2899 (2005).

[19] V. Rodionov, H. F. Gao, S. Scroggins, D. A. Unruh, A. J. Avestro, J. M. J. Fréchet, *J. Am. Chem. Soc*., **132**, 2570 (2010).

[20] F. Zhang, H. Jiang, X. Li, X. Wu, H. Li, *ACS Catal*., **4**, 394 (2014)

[21] E. L. Margelefsky, R. K. Zeidan, M. E. Davis, *Chem. Soc. Rev*., **37**, 1118, (2008).

[22] E. Angeletti, C. Canepa, G. Martinett, P. Venturello, *J. Chem. Soc*., **1**, 105 (1989).

[23] R. K. Zeidan, S. J. Hwang, M. E. Davis, *Angew. Chem. Int. Ed*., **45**, 6332 (2006).

[24] S .L. Hruby and B.H. Shanks, *J. Catal*., **263**, 181(2009).

[25] T. Toyao, M. Fujiwaki, Y. Horiuchi, M. Matsuoka, *RSC Adv*., **3**, 21582 (2013).

[26] R. K. Zeidan, S. J. Hwang, M. E. Davis, *Angew. Chem. Int. Ed*., **45**, 6332 (2006).

[27] S.L. Hruby, B.H. Shanks, *J. Catal*., **263**, 181 (2009).

[28] T. Toyao, M. Fujiwaki, Y. Horiuchi, M. Matsuoka, *RSC Adv*., **3**, 21582 (2013).

[29] F. Zhang, H. Jiang, X. Li, X. Wu, H. Li, *ACS Catal*., **4**, 394 (2014).

[30] Darui Wang, Bo Wang, Yu Ding, Haihong Wu, Peng Wu, ChemComm, **52**, 12817 (2016).

[31] S. Mondal, S. Sudhu, S. Bhattacharya, S. K. Saha, *J. Phys. Chem. C*, **119**, 27749 (2015).

[32] F. Tuinstra, J. L. Koenig, *J. Chem. Phys.*, **53**, 1126 (1970).

[33] M. M. Sk, C. Y. Yue, *RSC Adv.*, **4**, 19908 (2014).

[34] D. Wang, Z. Li, *Catal. Sci. Technol.*, **5**, 1623 (2015).

[35] H.-J. Shin, K. K. Kim, A. Benayad, S.-M. Yoon, H. K. Park, I.-S. Jung, M. H. Jin, H.-K. Jeong, J. M. Kim, J.-Y. Choi, Y. H. Lee, *Adv. Funct. Mater.*, **19**, 1987 (2009).

[36] S. Moussa, A. R. Siamaki, B. F. Gupton, M. S. El-Shall, *ACS Catal.*, **2**, 145 (2012).

[37] Z.-J. Fan, W. Kai, J. Yan, T. Wei, L.-J. Zhi, J. Feng, Y. Ren, L.-P. Song,

F. Wei, *ACS Nano*, **5**, 191 (2011).

[38] F. Zhang, H. Jiang, X. Wu, Z. Mao, H. Li, *ACS Appl. Mater. Interfaces* 7, 1669 (2015).

[39] H. Reinsch, M. A. van der Veen, B. Gil, B. Marszalek, T. Verbiest, D. de Vos, N. Stock, *Chem. Mater.*, **25**, 17 (2013).

[40] D. Wang, Z. Li, *Catal. Sci. Technol.*, **5**, 1623 (2015).